CF_3 Rotation in 3-(Trifluoromethyl)phenanthrene: Solid State ^{19}F and ^{1}H NMR Relaxation and Bloch−Wangsness−Redfield Theory

Peter A. Beckmann,*,†,‡ Jessie Rosenberg,†,§ Kerstin Nordstrom,†,# Clelia W. Mallory,||,⊥ and Frank B. Mallory⊥

Department of Physics and Department of Chemistry, Bryn Mawr College, 101 North Merion Avenue, Bryn Mawr, Pennsylvania 19010-2899, Department of Chemistry and Biochemistry, University of Delaware, Newark, Delaware 19716-2522, and Department of Chemistry, University of Pennsylvania, Philadelphia, Pennsylvania 19104-6323

Received: November 16, 2005; In Final Form: January 1, 2006

We have observed and modeled the ^{1}H and ^{19}F solid-state nuclear spin relaxation process in polycrystalline 3-(trifluoromethyl)phenanthrene. The relaxation rates for the two spin species were observed from 85 to 300 K at the *low* NMR frequencies of $\omega/2\pi = 22.5$ and 53.0 MHz where CF_3 rotation, characterized by a mean time τ between hops, is the only motion on the NMR time scale. All motional time scales ($\omega\tau \ll 1$, $\omega\tau \approx 1$, and $\omega\tau \gg 1$) are observed. The ^{1}H spins are immobile on the NMR time scale but are coupled to the ^{19}F spins via the unlike-spin dipole−dipole interaction. The temperature dependence of the observed relaxation rates (the relaxation is biexponential) shows considerable structure and a thorough analysis of Bloch−Wangsness−Redfield theory for this coupled spin system is provided. The activation energy for CF_3 rotation is 11.5 ± 0.7 kJ/mol, in excellent agreement with the calculation in a 13-molecule cluster provided in the companion paper where the crystal structure is reported and detailed ab initio electronic structure calculations are performed [Wang, X.; Mallory F. B.; Mallory, C. W; Beckmann, P. A.; Rheingold, A. L.; Francl, M. M *J. Phys. Chem. A* **2006**, *110*, 3954].

1. Introduction

We report ^{1}H and ^{19}F spin−lattice relaxation rate measurements as a function of temperature at two *low* NMR frequencies in 3-(trifluoromethyl)phenanthrene.

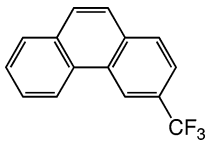

The low frequencies are necessary in NMR relaxation studies to bring the CF_3 group mean hopping rate τ^{-1} into resonance with the ^{1}H and ^{19}F NMR frequencies, as well as with the difference between the two NMR frequencies. This is in stark contrast to NMR spectroscopy where the drive is to higher and higher frequencies to better resolve chemical shifts and other interactions. The experiments and their analyses (section 4) provide an excellent test of the much-used Bloch−Wangsness−Redfield theory (section 2) for nuclear spin relaxation. This theory has been well tested for like-spin spin-1/2 systems such as ^{1}H. An extensive search of the literature (section 3) reveals several examples of unlike-spin spin-1/2 systems (usually, but not always, ^{1}H and ^{19}F) but the systems studied involve either more than one motion or limited dynamical regimes. In all cases known to us, this results in only a partial application (and therefore a partial test) of the theory. We are also able to compare the fitted NMR relaxation parameters presented here with those computed from knowing the crystal structure and from carrying out detailed ab initio electronic structure calculations, in both the isolated molecule and a 13-molecule cluster (section 5). These calculations are provided in the accompanying paper.[1] We conclude with general remarks (section 6).

2. Bloch−Wangsness−Redfield Relaxation Theory

We use the Bloch−Wangsness−Redfield theory of nuclear spin relaxation.[2−4] It is presented by Abragam (chapter 8),[5] Slichter (chapter 5),[6] Ernst et al. (chapter 2),[7] and Kimmich (chapter 11).[8] This perturbation theory approach has withstood the test of time, it has recently been presented in a broader context,[9] and its results can even be developed using a nonperturbative approach.[10] The perturbation Hamiltonian in the present case involves both the like-spin ($^{19}F-^{19}F$) and unlike-spin ($^{19}F-^{1}H$) spin−spin dipolar interactions. These interactions are modulated by CF_3 rotation.

In the nuclear spin relaxation experiments reported here, the magnetization of one of the two spin species is perturbed and its recovery to equilibrium monitored. The relaxation follows

* Corresponding author. E-mail pbeckman@brynmawr.edu.
† Department of Physics, Bryn Mawr College.
‡ Department of Chemistry and Biochemistry, University of Delaware.
§ Current address: Department of Applied Physics, California Institute of Technology, 1200 E. California Blvd. Mail Code 128-95, Pasadena, CA 91125-9500.
# Current address: Department of Physics and Astronomy, University of Pennsylvania, 209 South 33rd Street, Philadelphia, PA 19104-6396.
|| Department of Chemistry, University of Pennsylvania.
⊥ Department of Chemistry, Bryn Mawr College.

10.1021/jp056643o CCC: $33.50
Published on Web 02/24/2006

$$\begin{pmatrix} M_H(\infty) - M_H(t) \\ M_F(\infty) - M_F(t) \end{pmatrix} = -\begin{pmatrix} R^L_{HH} & 0 \\ 0 & R^L_{FF} \end{pmatrix}\begin{pmatrix} M_H(\infty) - M_H(t) \\ M_F(\infty) - M_F(t) \end{pmatrix} - \begin{pmatrix} R^U_{HH} & R^U_{HF} \\ R^U_{FH} & R^U_{FF} \end{pmatrix}\begin{pmatrix} M_H(\infty) - M_H(t) \\ M_F(\infty) - M_F(t) \end{pmatrix} \quad (1)$$

for magnetization $M_k(t)$ and equilibrium magnetization $M_k(\infty)$ (k = H or F). The first term in eq 1 with the diagonal relaxation rates is the usual single-species single-exponential relaxation equation.[5] The second term in eq 1 describes the relaxation of both species resulting from the unlike-spin H−F dipolar interactions. (This second term in eq 1 is eq 87, p 295 in Abragam,[5] where it is developed in detail.) The superscipts on the relaxation rates in the relaxation matrices refer to like (L) or unlike (U) spin−spin interactions. The subscripts refer to the position of the relaxation rate in the appropriate 2 × 2 matrix in eq 1. The like-spin ^{1}H spin−lattice relaxation rate R^L_{HH} results from the modulation of H−H dipolar interactions, the like-spin ^{19}F spin−lattice relaxation rate R^L_{FF} results from the modulation of F−F dipolar interactions and the unlike-spin ^{1}H−^{19}F spin−lattice relaxation rates R^U_{HH}, R^U_{HF}, R^U_{FH}, and R^U_{FF} all result from the modulation of H−F dipolar interactions.

For either ^{1}H or ^{19}F relaxation in a polycrystalline sample of 3-(trifluoromethyl)phenanthrene with a unique CF_3 environment in the structure,[1] there is only one motion on the NMR time scale, the reorientation of the unique CF_3 group. It follows that R^L_{HH} is identically zero and that there is only one correlation time τ that can be taken to be the mean time between CF_3 $2\pi/3$ hops in a Poisson process. The relaxation rates in the second row of the two relaxation matrices in eq 1 are

$$R^L_{FF} = R^{Lintra}_{FF} + R^{Linter}_{FF} = K^{Lintra}_{FF}\{J(\omega_F,\tau) + 4J(2\omega_F,\tau)\} + K^{Linter}_{FF}\{J(\omega_F,\tau/2) + 4J(2\omega_F,\tau/2)\} \quad (2)$$

$$R^U_{FF} = K^U_{FF}\{J(\omega_H-\omega_F,\tau) + 3J(\omega_F,\tau) + 6J(\omega_H+\omega_F,\tau)\} \quad (3)$$

and

$$R^U_{FH} = K^U_{FH}\{-J(\omega_H-\omega_F,\tau) + 6J(\omega_H+\omega_F,\tau)\} \quad (4)$$

It is convenient to separate the intramolecular (the same as intra-CF_3 in this case) and intermolecular parts for R^L_{FF}, but not for R^U_{FF} and R^U_{FH}, both of which have both intramolecular and intermolecular contributions, but the latter dominate. The relaxation rates in the first row of the two relaxation matrices in eq 1 are obtained by interchanging F and H in eqs 2−4 (except that $\tau = \infty$ for R^L_{HH} in eq 2, which makes $R^L_{HH} = 0$). The first term of eq 2 refers to the modulation of intra-CF_3 F−F interactions. The second term of eq 2 refers to the modulation of inter-CF_3 F−F interactions. Because the two F atoms are in different CF_3 groups for the second term, and because each CF_3 group is randomly reorienting with a mean frequency τ^{-1}, the modulation of these inter-CF_3 F−F interactions will be characterized by a mean frequency $2\tau^{-1}$.

The K values in eqs 2−4 come from the Bloch−Wangsness−Redfield theory with minor modifications for the current study as indicated in the following paragraphs.

$$K^{Lintra}_{FF} = \frac{1}{5}\frac{6}{3}\left(\frac{\mu_o}{4\pi}\right)^2 I_F(I_F+1)\gamma_F^4\hbar^2\frac{\Lambda(\theta_{FFintra})}{r^6_{FFintra}} = \frac{9}{40}\left(\frac{\mu_o}{4\pi}\right)^2\frac{\gamma_F^4\hbar^2}{r^6_{FFintra}} = (9.51\times10^8\ s^{-2}) = B \quad (5)$$

$$K^{Linter}_{FF} = \frac{1}{5}\left(\frac{\mu_o}{4\pi}\right)^2 I_F(I_F+1)\gamma_F^4\hbar^2\left[\frac{1}{3}\sum_{FFinter}\left(\frac{\Lambda(\theta_{FFinter})}{r^6_{FFinter}}\right)\right] = \frac{2}{3}K^{Lintra}_{FF}\left[\frac{1}{3}\sum_{FFinter}\Lambda(\theta_{FFinter})\frac{r^6_{FFintra}}{r^6_{FFinter}}\right] = yB \quad (6)$$

$$K^U_{FF} = \frac{1}{5}\frac{1}{3}\left(\frac{\mu_o}{4\pi}\right)^2 I_H(I_H+1)\gamma_H^2\gamma_F^2\hbar^2\frac{\Lambda(\theta_{HF})}{r^6_{HF}} = \frac{1}{20}\left(\frac{\mu_o}{4\pi}\right)^2\gamma_H^2\gamma_F^2\hbar^2\frac{\Lambda(\theta_{HF})}{r^6_{HF}} = \frac{2}{9}\left(\frac{\gamma_H}{\gamma_F}\right)^2\left\langle\left(\frac{r_{FFintra}}{r_{HF}}\right)^6\Lambda(\theta_{HF})\right\rangle B = \langle q_{HF}\rangle B = qB \quad (7)$$

and

$$K^U_{FH} = \frac{1}{5}\frac{1}{3}\left(\frac{\mu_o}{4\pi}\right)^2 I_F(I_F+1)\gamma_H^2\gamma_F^2\hbar^2\frac{\Lambda(\theta_{HF})}{r^6_{HF}} = \frac{1}{20}\left(\frac{\mu_o}{4\pi}\right)^2\gamma_H^2\gamma_F^2\hbar^2\frac{\Lambda(\theta_{HF})}{r^6_{HF}} = \frac{2}{9}\left(\frac{\gamma_H}{\gamma_F}\right)^2\left\langle\left(\frac{r_{FFintra}}{r_{HF}}\right)^6\Lambda(\theta_{HF})\right\rangle B = \langle q_{HF}\rangle B = qB \quad (8)$$

K^U_{HH} and K^U_{HF} are obtained by interchanging H and F in eqs 7 and 8.

The ^{1}H magnetogyric ratio is $\gamma_H = 2.675\times10^8\ s^{-1}\ T^{-1}$, the ^{19}F magnetogyric ratio is $\gamma_F = 2.517\times10^8\ s^{-1}\ T^{-1}$, $\mu_o/4\pi = 10^{-7}\ N\ A^{-2}$ where μ_o is the magnetic constant, $I_H = I_F = 1/2$ is the spin of both the ^{1}H and ^{19}F nucleus, the F−F distance in the CF_3 group is $r_{FFintra}$, the intermolecular F−F distances are $r_{FFinter}$, and r_{HF} is a *single* fluorine−proton distance discussed below. The parameter $\Lambda(\theta)$ in eqs 5−8 is

$$\Lambda(\theta) = \frac{3}{4}(\sin^4\theta + \sin^2 2\theta) \quad (9)$$

where θ is the angle between the fixed molecular rotation axis of the CF_3 group and the appropriate spin−spin vector. Equation 9 is part of eq 27 in Beckmann[11] where its inclusion in the first line of eq 5 is derived rigorously. In a polycrystalline sample, there is a random distribution of orientations of CF_3 rotation axes with respect to the magnetic field. This latter averaging results in a factor of 1/5 in the first lines of eqs 5−8.

For a single CF_3 group there are 6 interactions involving 3 spins and this is the origin of the factor 6/3 in the first line of eq 5. It is important that all spin pairs have the same fixed separation and identical motions to include more than a single interaction in such a simple numerical manner. Otherwise, a sum must be performed, as indicated in eq 6. The factor 1/3 in the brackets of both lines of eq 6 allows us to sum over the

intermolecular FF interactions involving all three F spins in a CF_3 group. In eqs 7 and 8 we assume a single effective unlike-spin dipolar interaction. Finally, the factors 1/3 in the first lines of eqs 7 and 8 have their origins in the quantum mechanical perturbation theory.[5]

The R_{FF}^{Lintra} part of eq 2, with eqs 5 and 9, can be obtained from Beckmann[11] eqs 11 and 12 with $N = 3$ and $L = 0$ (i.e., one term in both sums) and with $(\mu_o/4\pi)^2$ inserted to give SI units. This is also the same as eq 105 on p 300 of Abragam[5] or eq 31 of Beckmann[11] [again with $(\mu_o/4\pi)^2$ inserted in this work to give SI units].

There are relatively few parameters. The F−F distance in the CF_3 group is taken to be $r_{FFintra} = 0.2174$ nm. This number comes from averaging the appropriate F−F distances in the CF_3 groups obtained from the X-ray diffraction data and ab initio electronic structure calculations.[1]

The parameter B introduced in eq 5 is just K_{FF}^{Lintra}. It reappears in the last line of eqs 6−8 because it is convenient to compare those terms with K_{FF}^{Lintra}. The parameter $\theta_{FFintra} = \pi/2$ in eq 5. The dimensionless parameter y is defined by eq 6 and is about 0.1 (section 4). It is a measure of the ratio of the two like-spin contributions to the relaxation process; that is, the ratio of the intermolecular (which is the same as inter CF_3) F−F spin−spin interactions to the intramolecular (the same as intra-CF_3) F−F interactions. The parameter $\langle q_{HF}\rangle \equiv q$ is defined by eqs 7 or 8, the last two lines of which are identical. The way we have set it up, the model only permits one value of $\vec{r}_{HF}$ and it is not exactly clear how to compute the parameter q, which we will use as a fitting parameter. The dimensionless parameter q is found to be about 0.6 (section 4). However, as a guide, we take an appropriately weighted average of the product $(r_{FFintra}/r_{HF})^6\Lambda(\theta_{HF})$ as indicated in eqs 7 and 8 by $\langle\rangle$. The problems with calculating this value are discussed in section 5. The angles $\theta_{FFinter}$ in eq 6 and θ_{HF} in eqs 7 and 8 are the angles that $\vec{r}_{FFinter}$ and $\vec{r}_{HF}$ make with the CF_3 rotation axis. These can all be computed from the X-ray diffraction data and ab initio electronic configuration calculations.[1]

The spectral density in eqs 2−4 contains all the time dependence of the motion and is, for a Poisson process,

$$J(\omega,\tau) = \frac{2\tau}{1+\omega^2\tau^2} \tag{10}$$

Note that the spectral density in eq 10 differs from that in both Abragam[5] and Beckmann[11] by a factor of 2. Equations 3, 4, 7, 8, and 10, with $\Lambda(\theta) = 1$ in eqs 7 and 8, are the same as eq 88 on p 295 of Abragam[5] when the different definitions of the spectral densities are accounted for. (See also eq 104 on p 300 of Abragam[5] and the relationships between spectral densities discussed elsewhere.[12]) Abragam[5] and Beckmann[11] review other important, more fundamental assumptions and Beckmann,[11] and Palmer et al.[13] reiterate these assumptions and put them into perspective for methyl group rotation.

The correlation time τ is taken to be the mean time between "events" (in this case reorientations of the three F−F vectors in a CF_3 group) in a Poisson process and is modeled by the Canonical Ensemble:[14]

$$\tau^{-1} = \tau_o^{-1}e^{-E/kT} \tag{11}$$

More realistic (and complex) models have been investigated by Clough and Heidemann.[15] Incorporating them is unnecessary and would constitute an overanalysis of the data.

It is convenient to relate the "infinite-temperature hop rate" τ_o^{-1} and the "effective activation energy" E in eq 11 as a guide to what constitutes a reasonable order-of-magnitude value for τ_o^{-1}. If the barrier is taken to be unormalized Dirac δ-functions of width zero and height E at the rotational angles 0, $2\pi/3$, and $4\pi/3$, then the classical kinetic energy at the top of the barrier is $E = (1/2)I\omega^2 = (1/2)I[2\pi/(3\tau_o)]^2$, where τ_o is the time taken to rotate $2\pi/3$ and

$$\tau_o^{-1} = \frac{1}{x}\left(\frac{3}{2\pi}\right)\left(\frac{2E}{I}\right)^{1/2} \tag{12}$$

where I is the moment of inertia for the rotor undergoing the Poissonian reorientation. The parameter x (=1 in the naive model) is simply inserted into eq 12 as a useful fitting parameter and has no place in the model. Another simple model for τ_o^{-1} is that it is an "attempt" frequency and, as such, can be associated with a vibrational (or librational) frequency. In a harmonic approximation[14] τ_o^{-1} is given by eq 12 with the factor $(2E/I)^{1/2}$ replaced with $(E/2I)^{1/2}$. These two models differ by a factor of 2, an amazingly *small* difference given the extreme difference in the *form* of the barriers. This just says, unfortunately, that τ_o is *extremely insensitive* to the form of the barrier. If measured (i.e., fitted) values of τ_o^{-1} and E are not related by eq 12 to within, e.g., an order of magnitude or two, then the dynamical model should be suspect. In solid 3-(trifluoromethyl)phenanthrene there is a unique CF_3 site[1] and we do not allow for more than one value of τ in the model. This places a very significant restraint on fitting the data.

Equation 1 means that the nuclear magnetizations $M_H(t)$ and $M_F(t)$ relax with two time constants;

$$\frac{M_k(\infty) - M_k(t)}{2M_k(\infty)} = \phi_{k1}e^{-\lambda_1 t} + \phi_{k2}e^{-\lambda_2 t} \tag{13}$$

for k = H, F. The factor 2 is solely for convenience for the case of a perturbation using a π-pulse. The amplitudes $\phi_{k\rho}$ depend on the initial conditions (i.e., on $M_k(0)$) but *the observed relaxation rates* λ_ρ *do not.* The rates are obtained by diagonalizing the relaxation matrix in eq 1 and are

$$\lambda_{1,2} = \frac{1}{2}[(R_{FF}^L + R_{FF}^U) + (R_{HH}^L + R_{HH}^U) \pm \sqrt{[(R_{FF}^L + R_{FF}^U) - (R_{HH}^L + R_{HH}^U)]^2 + 4R_{FH}^U R_{HF}^U}] \tag{14}$$

If the protons are being observed and a π-pulse inverts the proton magnetization (i.e., $M_H(0) = -M_H(\infty)$), the amplitudes of the observed magnetization in eq 13 are

$$\phi_{H1} = 1 - \phi_{H2} = \frac{R_{HH}^L + R_{HH}^U - \lambda_2}{\lambda_1 - \lambda_2} \tag{15}$$

If F is the observed nucleus and a π-pulse is applied to the F magnetization, then *all* F's and H's are interchanged in eq 15.

We note that spin diffusion does not play a *direct* role in the model as we have set it up and this is somewhat counterintuitive. Spin diffusion does play an *indirect* role in that spin diffusion in the ^1H species will play a role in the value of q in eqs 7 and 8, as discussed further in section 5. For single species relaxation, the relaxation rate is often presented as the relaxation rate for a mobile group (like, e.g., a CH_3 group) diluted by (i.e., multiplied by) the ratio of the number of "relaxing" spins (three for a CH_3 group) to the total number of spins. This dilution ratio accounts for spin diffusion but does not appear anywhere here. For R_{FF}^L in the first term of eq 1, all ^{19}F nuclei appear in identical CF_3 groups. There are no other ^{19}F nuclei and so spin

diffusion plays no role in the determination of R^{L}_{FF}. For ^{1}H, R^{L}_{HH} in the first term of eq 1 is identically zero and so spin difusion plays no role here either. Spin diffusion plays an important role for the ^{1}H spin system in ensuring that the ^{1}H spin reservoir is always characterized by a common spin temperature. Indeed, the ^{19}F spin reservoir is also always characterized by a common spin temperature, although one that can be quite different from the ^{1}H spin system soon after a perturbation to one spin species but not the other. These common spin temperatures are ensured by noting that the observed values of $(T_2)_H$ and $(T_2)_F$ are much less than the observed λ_1^{-1} or λ_2^{-1}. It is important to note that as counterintuitive as it may seem, from the theoretical point of view, thinking of ^{1}H observed relaxation rates and ^{19}F observed relaxation rates is not helpful here. There are two observed relaxation rates: λ_1 and λ_2. The strong unlike-spin couplings force both spin species to relax with these same two rates.

3. Previous Work on the Two-Species Relaxation Problem

As is often the case, we were guided in this study by some beautiful experiments and some very lucid discussions presented, in this case, between 1961 and 1992. Abragam's 1961 pièce de résistance[5] is the beginning of truly understanding the theory with unlike-spin interactions included. The first experiment we could find was 1965, and this exceptional work[16] is discussed below.

In the liquid state, both the dipolar interaction *and* the spin-rotation interaction can be present, with the latter even being the dominant mechanism for ^{19}F relaxation.[17−19] Indeed, the spin-rotation interaction can even dominate for ^{1}H relaxation in the gaseous state.[20] However, dipolar interactions completely dominate for both ^{1}H and ^{19}F for polycrystalline van der Waals molecular solids.

Most prior work in solids has been done in ionic systems. Both ^{19}F and ^{1}H relaxation rates were measured[21] in NH_4PF_6. There is both PF_6^- and NH_4^+ rotation and the authors were able to observe biexponential relaxation in the slow-motion limit of PF_6^- rotation. The details are complicated by the fact that this occurs at the onset of NH_4^+ rotation. ^{19}F and ^{1}H relaxation measurements[22] in NH_4HF_2 showed complex behavior similar to that found in NH_4PF_6. Again, there are different motions in different regimes and at high temperatures the ^{19}F and ^{1}H magnetizations are not coupled and relax independently. Thus two separate applications of the theory for like-spin systems are applied at high temperature and, somewhat independently, the theory for the two-spin unlike-spin system is applied at low temperature.

Bloch−Wangsness−Redfield theory can certainly be applied to spins with $I > 1/2$ and a beautiful study[23] of ^{13}C relaxation in KCN and NaCN makes an important point. Whereas ^{13}C has $I = 1/2$, ^{23}Na (100% abundance) and ^{39}K (93% abundance) have $I = 3/2$. When $\omega_C/2\pi = 24.15$ MHz, $\omega_{Na}/2\pi = 26.45$ MHz and $\omega_K/2\pi = 4.67$ MHz. Thus in the ^{13}C relaxation rate versus temperature plot, the effects of cross relaxation with the quadrupolar ^{23}Na spin species are observable for NaCN (where the difference in the two NMR frequencies is 2.3 MHz) but the effects of cross relaxation with the quadrupolar ^{39}K spin species are *not* observable in KCN (where the difference frequency is 19.5 MHz). This paper has a very clear discussion of Bloch−Wangsness−Redfield theory and how it applies when dipole−dipole and chemical shift anisotropy interactions are both present (^{13}C relaxation in KCN), and when quadrupolar interactions (^{23}Na) and dipolar interactions (^{13}C relaxation in NaCN) are both present. The ^{13}C relaxation rate versus T plot also shows the relaxation rate maximum when $(\omega_{Na} - \omega_C)\tau$ is of order unity due to the first term in our eqs 3 and 4.

In a thorough study,[24] the basic Bloch−Wangsness−Redfield theory for a two-spin species system was applied to a well-studied complex: $H_3N{:}BF_3$. Very slight departures from exponential relaxation were observed and single rates were extracted from initial slopes of the magnetization recoveries. The same authors followed with a more complex ionic system[25] in which the cation, containing four mobile CH_3 groups, was obtained by one-electron oxidation of *N,N,N′,N′*-tetramethyl-*p*-phenylenediamine, and the counterion was BF_4^-. Both the ^{19}F and ^{1}H magnetizations relaxed largely exponentially in a situation where the modulations of different interactions were responsible for ^{19}F and ^{1}H relaxation: hyperfine interactions for the former and dipolar electron−nuclear interactions for the latter. In both these studies and some of those mentioned previously, the H − F distances are too great to result in significant nonexponential relaxation. This was also found to be the case[26] in the complex $FeSiF_6{\cdot}6H_2O$.

In the ionic system $[Sb(CH_3)_4]PF_6$, complicated relaxation rate versus temperature plots for ^{19}F and ^{1}H contain a wealth of information, in principle, but in practice, there are too many motions and the ^{19}F and ^{1}H nuclei are too far apart (to provide a significant test of Bloch−Wangsness−Redfield theory).[27] $[Sb(CH_3)_4]^+$ rotation is seen at high temperatures and three types of PF_6^- rotation (uniaxial reorientation, isotropic reorientation, and translational motion) are seen over a wide temperature range. In addition, the ^{31}P resonance is too far from the ^{19}F and ^{1}H resonance for cross relaxation to have much effect. Nonexponential relaxation was only seen over a very small temperature range at very low temperatures where the ^{19}F and ^{1}H nuclei could communicate effectively with each other. The experiments, however, were a tour de force.

A few important studies have been conducted in van der Waals molecular crystals such as that studied here, but not many. One of the earliest observations (1965) of both ^{19}F and ^{1}H relaxation was in the three compounds $C_6H_5CF_3$, *m*-$C_6H_4(CF_3)_2$, and *p*-$C_6H_4(CF_3)_2$.[16] These room-temperture liquids were studied in the solid state over the temperature ranges 105−195, 88−190, and 90−160 K, respectively. Although the authors were unable to measure specific rates with the apparatus available at that time, they noted "null points" in magnetization recovery experiments and presented a beautiful discussion that contains the essence of much of the application of Bloch−Wangsness−Redfield theory to these kinds of systems. Our review of the literature suggests that this paper is, in some sense, the beginning of this experimental field.

In a very interesting system, solid 1,3,5-trifluorobenzene, the low-temperature biexponential regime was observed, with both ^{19}F and ^{1}H relaxing with the same two relaxation rates.[28] The magnetization fractions relaxing with each rate were 50%, as must be the case in the low-temperature limit for this system. Indeed, in this case, interchanging H's and F's gives an identical molecular system. This experiment was a beautiful test case of Bloch−Wangsness−Redfield theory in the low-temperature regime.

A very thorough and helpful study[29] has been presented in the molecular solid CHF_3 over the temperature range from 70 to 120 K. Here, the crystal structure is known and the authors were able to interpret the relaxation in terms of the modulation of H−H, F−F, and F−H interactions resulting from 3-fold rotation about the C−H axis of the molecules. The authors were only really able to observe in the low-temperature regime and

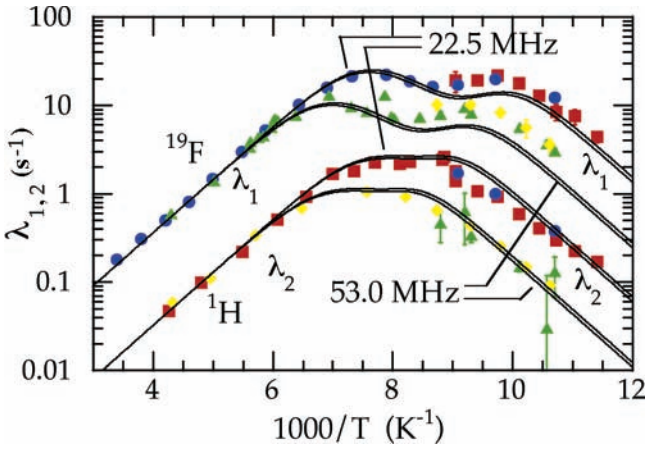

Figure 1. Observed spin−lattice relaxation rates λ_1 and λ_2 versus inverse temperature T^{-1}: λ_{1F} and λ_{2F} at 22.5 MHz (circles [blue online]); λ_{1F} and λ_{2F} at 53.0 MHz (triangles [green online]); λ_{1H} and λ_{2H} at 22.5 MHz (squares [red online]); λ_{1H} and λ_{2H} at 53.0 MHz (diamonds [yellow online]). Where error flags are not shown, they are within the size of the symbols. Where the same symbol is used for both λ_{1k} and λ_{2k} (k = H, F), the two rates are sufficiently distinct as to not be confused. The relaxation is exponential within experimental uncertainty for 1000 T^{-1} < 8.9 K^{-1} (T > 110 K) with ^{19}F relaxing with λ_1 and ^{1}H relaxing with λ_2. The relaxation is biexponential within experimental uncertainty for 1000 T^{-1} > 8.9 K^{-1} (T < 110 K) and is independent of the nucleus; that is $\lambda_{jF} = \lambda_{jH}$ for j = 1, 2. The several lines are a single fit with four adjustable parameters as discussed in the text.

in the vicinity of a relaxation rate maximum. Whereas they did observe the ^{1}H magnetization relaxing with both rates, they were only able to observe exponential ^{19}F relaxation with the single rate being the lower of the two ^{1}H rates. An interesting aspect of this study is that the authors tried to correlate the intensities of the various rates (i.e., the K-values in eqs 2−4) with second moment measurements, though they treated the second moments as parameters in their fits of the data. We present a simpler system in this paper and we have calculated the dominant constant, K_{FF}^{Lintra} in eq 5 explicitly. It is not a fitting parameter.

4. Relaxation Rate Experiments and Their Analysis

The fluorine-19 (^{19}F) and proton (^{1}H) spin−lattice relaxation rates λ_{ik} (i = 1, 2; k = F, H) were measured as a function of temperature T at two Larmor frequencies: $\omega_k/2\pi$ = 22.5 and 53.0 MHz. (The rates λ_{ik} are independent of nucleus k but we still need to keep the data separate.) The experiments are fixed frequency, *not* fixed field. For $\omega/2\pi$ = 53.0 MHz, B_H = 1.24 T and B_F = 1.32 T. For $\omega/2\pi$ = 22.5 MHz, B_H = 0.527 T and B_F = 0.560 T. The λ_{ik} were measured using a standard inversion−recovery sequence ($\pi-t-\pi/2-$observe$-t_o$) with t_o > 8 times the largest value of λ_{ik}^{-1}.

Temperature was varied by means of a flow of cold nitrogen gas and temperature was measured with a carefully home-silver-soldered, calibrated copper−constantan thermocouple. The data are shown in Figure 1. The relaxation is exponential within experimental uncertainty above 110 K ($1000T^{-1} < 8.9K^{-1}$) with ^{19}F relaxing with λ_1 and ^{1}H relaxing with λ_2. Measuring these rates to an uncertainty of ±5% is straightforward. The biexponential relaxation below 110 K ($1000T^{-1} > 8.9K^{-1}$) is more time-consuming to characterize accurately, especially for the smaller λ_2 values for ^{19}F (lower triangles in Figure 1). The uncertainties, in some cases, are considerable. The lowest-temperature ^{19}F measurement is shown in Figure 2.

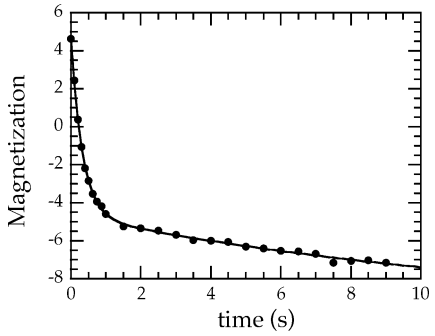

Figure 2. ^{19}F magnetization versus time t at T = 93.5 K (1000/T = 10.7 K^{-1}). The wait time in the inversion−recovery experiment ($\pi-t-\pi/2-$observe$-t_o$) is t_o = 60 s, which is $7.8\lambda_{2F}^{-1}$. Four scans were collected for each t value, and the experiment took 2 h. The five-parameter Simplex fit gives λ_{1F} = 3.01 ± 0.02 s^{-1}, λ_{2F} = 0.13 ± 0.06 s^{-1}, ϕ_{1F} = 0.71 ± 0.05, ϕ_{2F} = 0.29 ± 0.07, and a = 0.6 ± 0.3. The last parameter is the effectiveness of the π-pulse. A perfect π-pulse corresponds to a = 1. These two data points are the lowest-temperature triangles in Figure 1.

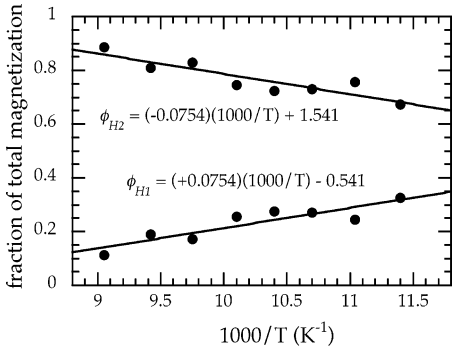

Figure 3. Observed values of ϕ_{H1} and ϕ_{H2} versus 1000/T. The linear fits provide a convenient guide for the eye and have no theoretical basis. The uncertainties are within the size of the symbols. Note that $\phi_{H1} + \phi_{H2}$ = 1 (exactly).

The observed relaxation rates are independent of nucleus; that is $\lambda_{jF} = \lambda_{jH}$ for j = 1, 2. This is not readily apparent from the data at high temperature in Figure 1. At low temperatures, where the relaxation is biexponential, this is apparent. However, as T increases, $\phi_{H1} \rightarrow 0$, $\phi_{H2} \rightarrow 1$, $\phi_{F1} \rightarrow 1$, and $\phi_{F2} \rightarrow 0$ in eq 13 as shown below. Thus, only one of the two rates can actually be observed, the relaxation is exponential with $\lambda_{F1} = \lambda_1$, $\lambda_{H2} = \lambda_2$, and λ_{F2} and λ_{H1} though, in principle present, cannot be measured because ϕ_{F2} and ϕ_{H1} are vanishingly small. In Figure 3, we show ϕ_{H1} and ϕ_{H2} as a function of temperature in the low-temperature, biexponential regime.

At high temperatures, $\omega_H\tau$, $\omega_F\tau$, $2\omega_F\tau$, $(\omega_H + \omega_F)\tau$, and $(\omega_H - \omega_F)\tau$ are all ≪1, where τ is the mean time for CF_3 $2\pi/3$ hops in a Poisson process. (The parameter $2\omega_H\tau$ does not enter the problem because H−H interactions are not modulated by CF_3 rotation.) This is the fast motion limit on all time scales. In this regime, $\ln(\lambda_j) = (E/k)T^{-1}$ + constant (with the constant being different for the two rates $\lambda_{1,2}$). Going down in temperature, there is a maximum when $\omega_H\tau$, $\omega_F\tau$, $2\omega_F\tau$, and $(\omega_H + \omega_F)\tau$ are all of order unity but $(\omega_H - \omega_F)\tau$ is still ≪1 or at least <1. Then there is another maximum at lower temperatures when $(\omega_H - \omega_F)\tau$ is of order unity and all the others are ≫1 or at least >1. These two maxima are most clearly resolved at 22.5 MHz. Finally, at low temperature, $\omega_H\tau$, $\omega_F\tau$, $2\omega_F\tau$, $(\omega_H + \omega_F)\tau$, *and* $(\omega_H - \omega_F)\tau$ are all ≫1 and $\ln(\lambda_j) = -(E/k)T^{-1}$ + constant for both rates (with the constant again being different for the

two rates $\lambda_{1,2}$). This is the slow-motion limit on all time scales. This explains the general shape of the relaxation curves in Figure 1.

We fit the data with four adjustable parameters that were determined to be $E = 11.5 \pm 0.7$ kJ/mol in eq 11, $x = 0.36 \pm 0.06$ in eq 12, $y = 0.10^{+0.10}_{-0.05}$ in eq 6, and $q = 0.055 \pm 0.010$ in eqs 7 and 8. The fit is relatively insensitive to the parameter y, as can be seen from the large percentage experimental uncertainty in that parameter. The slopes of the high and low-temperature $\ln(\lambda_1)$ or $\ln(\lambda_2)$ versus $1/T$ plots (both frequencies) are equal and opposite and uniquely determine the activation energy E independently of the other parameters. The remaining fit can then be considered a three-parameter fit to determine x, y, and q.

We define the parameter Q by

$$Q = \left(\frac{q}{1 + \frac{1}{2}y}\right) \ll 1 \qquad (16)$$

For the magnetizations at high temperature, it can be shown that to order Q^3, eq 15 can be written

$$\varphi_{F1} = 1 - \varphi_{F2} = \varphi_{H2} = 1 - \varphi_{H1} = 1 - Q^2 \qquad (17)$$

It then follows from eq 13 that the relaxation is exponential with the ^{19}F magnetization relaxing with λ_1 and the ^{1}H magnetization relaxing with λ_2.

Finally, we note, for curiosity's sake, that in the theoretical fits, the difference in the relaxation terms in $\omega_H - \omega_F$ when observing ^{1}H and when observing ^{19}F (i.e., the difference between 2π[3.139 MHz] when observing ^{1}H and 2π[3.336 MHz] when observing ^{19}F) lead to the two closely spaced lines in the middle and low temperatures in Figure 1. The difference between these two difference frequencies is 6% and λ_j at the lowest temperatures is proportional to $(\omega_H - \omega_F)^{-2}$. This very small difference cannot be distinguished in the experimental relaxation rates.

5. Comparing the Fitted and Computed Values of *E*, *x*, *q*, and *y*

The observed effective activation energy for CF_3 rotation is $E = 11.7 \pm 0.7$ kJ/mol. Extensive ab initio electronic structure calculations based on the crystal structure are performed in the accompanying paper.[1] The barrier height has both intramolecular and intermolecular contributions. The former is computed to be 2 kJ/mol and the two together are computed to be 11 kJ/mol. Although a barrier height is not quite the same physical quantity as an observed effective activation energy in an NMR relaxation experiment, they are close and the agreement between the computed value and the experimental value reported here is reassuring.

The values of x and E fix the mean time between hops τ for the CF_3 group via eqs 11 and 12. The value of $x = 0.36 \pm 0.06$ simply suggests that the assumption that CF_3 rotation is responsible for the relaxation is reasonable. If x were several orders of magnitude from unity, this would be difficult to explain. Because models for τ are so insensitive to the fitted value of τ_o, this agreement serves only as an "order-of-magnitude" check on the meaningfulness of the model.

The fitted parameter $y = 0.10^{+0.10}_{-0.05}$ is a measure of the intermolecular (and therefore inter-CF_3 group) FF dipolar interactions. This range in y values means that these interactions contribute between 5 and 20% of the relaxation coming from intramolecular (and therefore intra-CF_3 group) FF dipolar interactions. These intermolecular spin−spin interactions should not be confused with, and have nothing to do with, the intermolecular interactions that dominate the barrier E. The dimensionless parameter y can be computed from eq 6. Using both the crystallography data and the ab initio calculations as described in the accompanying paper,[1] we have computed y using the nearest 36 F atoms to each of the three F atoms in a CF_3 group, for a total of 108 intermolecular FF interactions. This computed value gives $y = 0.111$, in good agreement with the albeit poorly determined experimental value. If we included only the 16 nearest FF distances, all of which are <0.5 nm, $y = 0.102$. Indeed, if we considered only the three nearest neighbors at 0.276, 0.303, and 0.303 nm, $y = 0.057$, more than half the observed total. We note for completeness that the factors $\Lambda(\theta_{FFinter})$ in eq 6 (and the factors $\Lambda(\theta_{HF})$ in eqs 7 and 8), and defined in eq 9, are all of order unity, ranging, in practice, from 0.4 to 1.0. (This parameter does range from 0 to 1, but only a small range of angles centered around 0 and π contribute to the range from 0 to 0.4.)

The dimensionless parameter q in eqs 7 and 8 is more difficult to relate to a computed quantity, but a crude calculation can be performed and is of the right order of magnitude. One is tempted to compute

$$\Theta = \frac{1}{3}\sum_{FH} q_{FH} = \frac{1}{3}\sum_{FH}\frac{2}{9}\left(\frac{\gamma_H}{\gamma_F}\right)^2\left(\frac{r_{FFintra}}{r_{HF}}\right)^6 \Lambda(\theta_{HF}) \qquad (18)$$

where q_{FH} is defined in eqs 7 and 8 and where the sum involves the relevant FH interactions for all three F spins in a CF_3 group. The factor 1/3 normalizes the sum to a "per F spin" interaction. On the average, each set of three F nuclei are interacting with nine H nuclei. The CF_3 groups are arranged in sheets[1] and many F spins are interacting with the H spins in and near those sheets. On top of this, both FF and HH spin diffusion is going to affect this process in ways that are difficult to model. Indeed, it is likely that one or two FH interactions are totally dominant for each F spin and that HH spin diffusion quickly equilibrates the H spin temperature.

The four largest individual $q_{FH}/3$ values in eq 18 (corresponding to the smallest values of r_{HF}) are 0.0294, 0.0201, 0.0195, and 0.0174, whose sum, 0.0864, can be compared with the observed value of $q = 0.055 \pm 0.010$. A sum over the nearest 10 r_{HF} distances gives $q_{FH}/3 = 0.17$. Because there are only three ^{1}H spins for each ^{19}F spin, simply adding the nearest ten F−H interactions represents "overcounting." Further work is needed here but it is not unreasonable to say that the theoretical model used to fit the data and the computations based on the crystal structure are of the same order of magnitude.

6. Concluding Remarks

We have measured ^{1}H and ^{19}F nuclear spin−lattice relaxation rates in solid 3-(trifluoromethyl)phenanthrene. The relaxation is exponential at high temperature and biexponential at low temperature. The temperature dependence of the rates at two NMR frequencies shows considerable detail, all of which has been modeled using Bloch−Wangsness−Redfield theory plus structural information provided by X-ray crystallography and appropriate F and H atom positions provided by ab initio electronic configuration calculations.[1] Applying Bloch−Wangsness−Redfield theory to these data results in a good quantitative understanding of the relaxation process. We have also developed a clear conceptual understanding of the relaxation process over the entire temperature range, which includes the high, fast-

motion and low, slow-motion temperature regimes, as well as the intermediate temperature regime that includes two maxima in the relaxation rates, even though there is only a single motion. To our knowledge, this is the only report of the measurement of the relaxation rates for unlike dipolar coupled nuclei in which *all* motional regimes have been investigated *both* experimentally and theoretically. We have included both intramolecular and intermolecular FF dipolar interactions and both intramolecular and intermolecular FH dipolar interactions. (HH interactions are not modulated by CF_3 rotation, the only motion on the NMR time scale.)

Bloch−Wangsness−Redfield theory has succeeded admirably, and although it was well-presented 45 years ago,[5] only by combining the observed relaxation rates of both spin species over all motional regimes with X-ray crystallography and ab initio electronic structure calculations with clusters of van der Waals molecules[1] can a thorough test of the theory be conducted.

References and Notes

(1) Wang, X.; Mallory, F. B.; Mallory, C. W.; Beckmann, P. A.; Rheingold, A. L.; Francl, M. M. *J. Phys. Chem. A* **2006**, *110*, 3954.

(2) Bloch, F. *Phys. Rev.* **1956**, *102*, 104−135; Bloch, F. *Phys. Rev.* **1957**, *105*, 1206−1222.

(3) Redfield, A. G. *IBM J. Res. Develop*. **1957**, *1*, 19−31, reprinted with minor revisions in *Adv. Magn. Reson.* **1965**, *1*, 1−32.

(4) Wangsness, R. K.; Bloch, F. *Phys. Rev.* **1953**, *89*, 728−739.

(5) Abragam, A. *The Principles of Nuclear Magnetism*; Oxford University Press: Oxford, U.K., 1961.

(6) Slichter, C. P. *Principles of Magnetic Resonance*, 3rd ed; Springer-Verlag: Berlin, 1990.

(7) Ernst, R. R.; Bodenhausen, G.; Wokaum, A. *Principles of Nuclear Magnetic Resonance in One and Two Dimensions*; Oxford University Press: Oxford, U.K., 1987.

(8) Kimmich, R. *NMR Tomography, Diffusometry, Relaxometry*; Springer-Verlag: Berlin, 1997.

(9) Kleinekathöfer, U. *J. Chem. Phys*. **2004**, *121*, 2505−2514.

(10) Fatkullin, N. Magnetic Resonance and Related Phenomena. Extended Abstracts of the XXVIIth Congress, Ampere, Kazan, 1994; p 235.

(11) Beckmann, P. A. *Mol. Phys.* **1980**, *41*, 1227−1238.

(12) Soda, G.; Chihara, H. *J. Phys. Soc. Jpn.* **1974**, *36*, 954−958.

(13) Palmer, C.; Albano, A. M.; Beckmann, P. A. *Physica B* **1993**, *190*, 267−284.

(14) Owen, N. L. In *Internal Rotation in Molecules*; Orville-Thomas, W. J., Ed.; Wiley: New York, 1974.

(15) Clough, S.; Heidemann, A. *J. Phys. C* **1980**, *13*, 3585−3589.

(16) Anderson, J. E.; Slichter, W. P. *J. Chem. Phys.* **1965**, *43*, 433−437.

(17) Namgoong, H.; Lee, J. W. *Bull. Korean Chem. Soc*. **1992**, *14*, 91−95.

(18) Huang, S.-G.; Rogers, M. T. *J. Chem. Phys.* **1978**, *68*, 5601−5606.

(19) Gutowsky, H. S.; Lawrenson, I. J.; Shimomura, K. *Phys. Rev. Lett.* **1961**, *6*, 349−351.

(20) Beckmann, P. A.; Bloom M.; Ozier I. *Can. J. Phys.* **1976**, *54*, 1712−1727.

(21) Albert, S.; Gutowsky, H. S. *J. Chem. Phys.* **1973**, *59*, 3585−3594.

(22) Reynhardt, E. C.; Watton, A.; Petch, H. E. *J. Chem. Phys.* **1979**, *71*, 4421−4429.

(23) Stokes, H. T.; Ailion, D. C.; Case, T. A. *Phys. Rev. B* **1984**, *30*, 4925−4934.

(24) Yamauchi, J.; McDowell, C. A. *J. Chem. Phys.* **1981**, *75*, 577−583.

(25) Yamauchi, J.; McDowell, C. A., *J. Chem. Phys.* **1981**, *75*, 1060−1068.

(26) Rager, H. *Z. Naturforsch.* **1981**, *36a*, 637−642.

(27) Burbach, G.; Weiden, N.; Weiss, A. *Z. Naturforsch.* **1992**, *47a*, 689−701.

(28) Albert, S.; Ripmeester, J. A. *J. Chem. Phys.* **1979**, *70*, 1352−1358.

(29) Watton, W.; Pratt, J. C.; Reynhardt, E. C.; Petch, H. E. *J. Chem. Phys.* **1982**, 77, 2344- 2349.